

# Temperature modulated differential scanning calorimetry. Part I: Effects of heat transfer on the phase angle in dynamic ADSC in the glass transition region<sup>1</sup>

Zhong Jiang<sup>a</sup>, Corrie T. Imrie<sup>a</sup>, John M. Hutchinson<sup>b,\*</sup>

<sup>a</sup> Department of Chemistry, University of Aberdeen, Aberdeen AB24 3UE, UK

<sup>b</sup> Department of Engineering, University of Aberdeen, Aberdeen AB24 3UE, UK

## Abstract

The relatively new technique of alternating differential scanning calorimetry (ADSC) relies upon the measurement of a phase angle between the heating rate and heat flow in order to separate the real and imaginary parts of the complex heat capacity. A significant problem in this context is the separation of an 'instrumental' phase angle, arising from the heat transfer between instrument and sample, from any 'sample' phase angle which may result from a transition. In this work, the theoretically anticipated dependence of phase angle on the frequency of modulation has been investigated experimentally for polycarbonate in dynamic scans through the glass transition region using the Mettler–Toledo ADSC. There is a good agreement between the experimental results and the predictions of simple models for both heat transfer and relaxation in the transition region. This provides support for the procedure originally suggested by Schick and co-workers for the correction of the phase angle to allow for the instrumental effects. © 1998 Elsevier Science B.V.

**Keywords:** Alternating DSC; Heat capacity; Phase angle; Glass transition; Polycarbonate

## 1. Introduction

In Alternating Differential Scanning Calorimetry (ADSC, Mettler–Toledo), the idea of modulating the constant heating rate of conventional DSC originally conceived by Reading [1–3] is adopted. The temperature  $T$  is programmed as a sinusoidal modulation of amplitude  $A_T$  and frequency  $\omega$  (rad s<sup>-1</sup>), around a constant rate of increase of temperature,  $\beta$ , from an initial temperature  $T_0$ , so the temperature can be described as:

$$T = T_0 + \beta t + A_T \sin(\omega t) \quad (1)$$

\*Corresponding author. Tel.: +44 1224 272791; fax: +44 1224 272497; e-mail j.m.hutchinson@eng.abdn.ac.uk

<sup>1</sup>Presented at TAC 97, Oxford, UK, 14–15 April 1997.

The heating rate is given by:

$$q = \beta + A_T \omega \cos(\omega t) \quad (2)$$

from which it can be seen that  $q$  is completely defined by  $\beta$ ,  $A_T$  and  $\omega$ , all of which can be changed independently. The most commonly used signal superimposed on the linear heating programme is sinusoidal (Fig. 1).

Using Schawe's formulation [4], the complex heat capacity ( $C_p^*$ ), in-phase heat capacity ( $C_p'$ ) and the out-of-phase heat capacity ( $C_p''$ ), are, respectively, defined as:

$$C_p^* = \frac{A_{HF}}{A_q} \quad (3)$$

$$C_p' = C_p^* \cos\phi \quad (4)$$

$$C_p'' = C_p^* \sin\phi \quad (5)$$

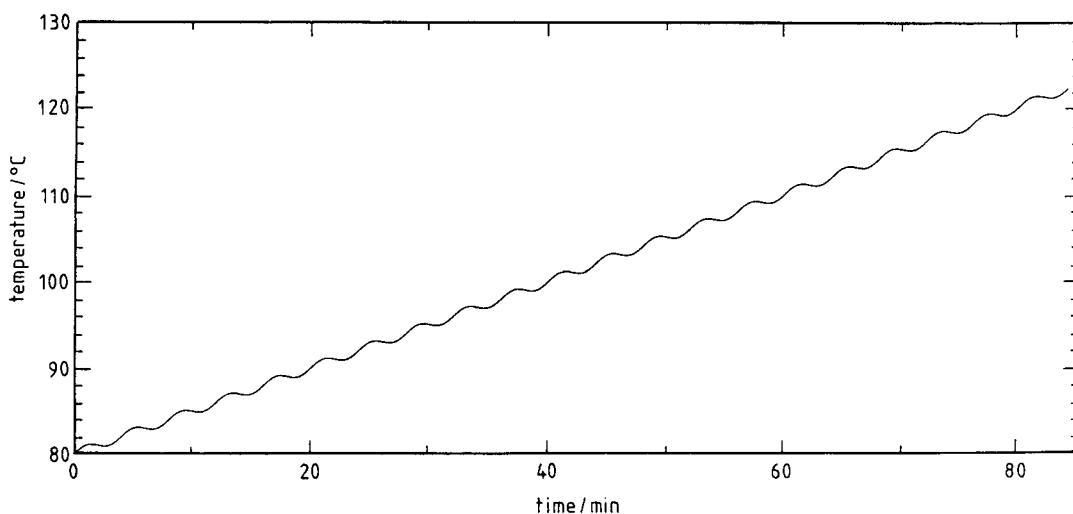


Fig. 1. Part of the ADSC temperature modulation programme used here in the study of the glass transition of polycarbonate. The experimental variables are: average heating rate,  $\beta=0.5$  K/min; amplitude,  $A_T=0.5$  K; period,  $p=4$  min or frequency,  $\omega=2\pi/240$  rad  $s^{-1}$ .

where  $A_{HF}$  is the amplitude of the heat flow modulations,  $A_q$  is the amplitude of the heating rate modulations and  $\phi$  is the phase angle.

The following features of the ADSC response, and of temperature modulated DSC in general, are observed in the glass transition region of polymers (refer to Fig. 2):

- *Complex heat capacity,  $C_p^*$* : The complex heat capacity shows a ‘step change’ of magnitude  $\Delta C_p^*$  in a temperature range which depends on the frequency of modulation. This temperature range can be specified by a ‘mid-point temperature’,  $T_{mid}$ , where the value of  $C_p^*$  is mid-way between the glassy and liquid-like asymptotes.
- *Phase angle,  $\phi$* : The phase angle shows a departure from its almost constant (non-zero, in practice) value in the glassy region at approximately the same temperature as the step change in  $C_p^*$ . This departure reaches a maximum value  $\Delta\phi_{max}$  before returning to a level different from the glassy state value. The change in phase angle through the transition region is identified as  $\Delta\phi$ .
- *In-phase heat capacity,  $C_p'$* : Because the phase angle is rather small, the in-phase heat capacity is very similar to  $C_p^*$ .

- *Out-of-phase heat capacity,  $C_p''$* : Similarly, because the phase angle is small and  $\Delta C_p^*$  is also small, the out-of-phase heat capacity closely follows the behaviour of the phase angle itself.

All of these features can be described qualitatively by a simple theoretical model [5,6] which considers the relaxation process in a glassy polymer in the glass transition region. Nevertheless, there are some important differences in detail between the theoretical predictions and experimental results such as those shown in Fig. 2. In particular, the phase angle is predicted to be zero before and after the transition and to deviate from zero only in the transition interval; the experimental results show clearly that the phase angle is not zero either before or after the transition and indeed has different non-zero values in the glassy and liquid-like regions. The reason for this lies in the additional effect of heat transfer between instrument and sample, which is not included in the current theoretical analysis, but which has an important influence on the phase angle. This was noted previously by Wunderlich et al. [7], but a systematic study of these effects is still required. In the present work, the theoretically anticipated dependence of phase angle on the frequency of modulation has been investigated experimentally for polycarbo-

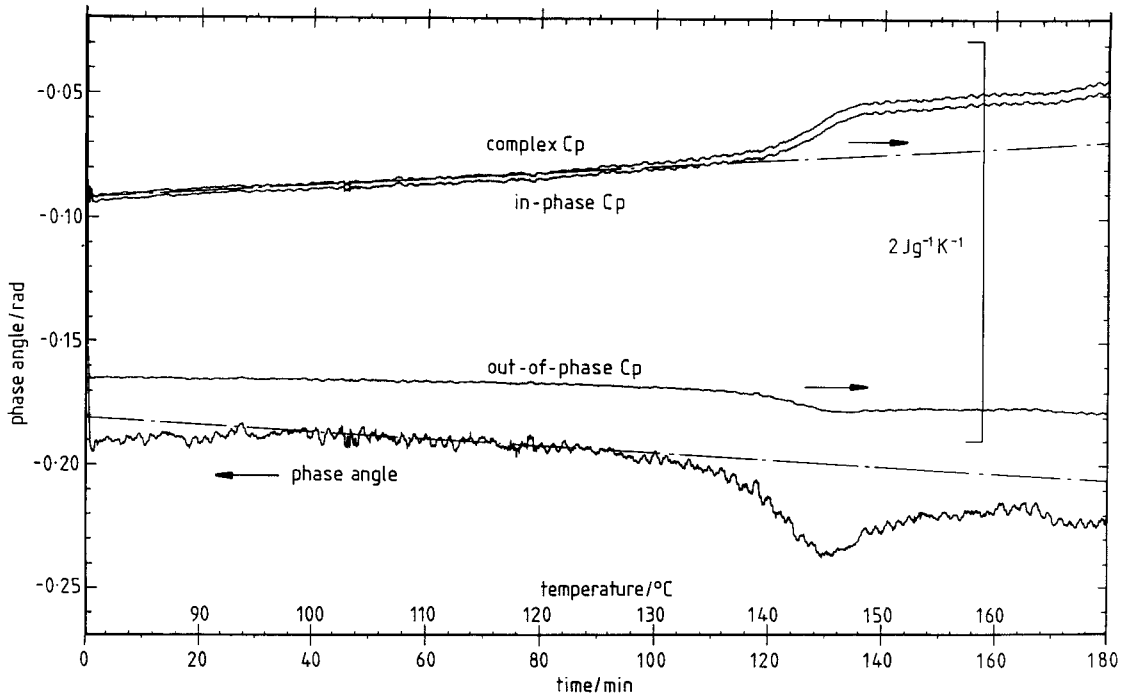


Fig. 2. Typical ADSC results for polycarbonate with  $\beta=0.5$  K/min,  $A_T=1$  K, period=1 min, from 80°C to 170°C. The heat capacities are on a relative scale (right hand scale bar) and have been displaced from each other for clarity. The phase angle is on an absolute scale (left hand axis). The dash-dotted lines correspond approximately to the asymptotic glassy behaviour. Note that the in-phase and out-of-phase specific heat capacities have been calculated using the uncorrected phase angle (see later).

nate in dynamic measurements using the Mettler–Toledo ADSC.

## 2. Theory of heat transfer in ADSC

The following analysis is due to Wunderlich et al. [7]. The rate of heat flow from DSC (temperature  $T_d$ ) to sample (temperature  $T$ ) is;

$$\frac{dQ}{dt} = K(T_d - T) \quad (6)$$

where  $K$  is the Newton's law constant. For a sinusoidal temperature modulation (Eq. (1)) this leads to the following differential equation for the heat flow:

$$\frac{dQ}{dt} = K\left(\beta + A_T \sin \omega t - \frac{Q}{mC_p}\right) \quad (7)$$

where  $m$  and  $C_p$  are the mass and specific heat of the sample, respectively.

This may be solved to give the steady state temperature modulation of the sample:

$$T - T_0 = \beta(t - \tau) + \frac{A_T}{\sqrt{1 + \omega^2 \tau^2}} \sin(\omega t - \phi_{HT}) \quad (8)$$

where  $\tau$  is a time constant given by:

$$\tau = \frac{mC_p}{K} \quad (9)$$

and  $\phi_{HT}$  is the phase angle due to heat transfer given by:

$$\phi_{HT} \approx \arctan(\omega\tau) = \arctan\left(\frac{mC_p\omega}{K}\right) \quad (10)$$

From this it can be seen that, for small phase angles,  $\phi_{HT}$  is linearly related to  $m$ ,  $C_p$  and  $\omega$ .

### 3. Experimental

#### 3.1. Materials

The polycarbonate samples were machined from a 40 mm diameter extruded solid rod (Tecanat, Ensinger). Smaller rods, with diameter 5 mm to suit the aluminium crucibles (pans) of the DSC, were turned and then parted on a lathe into discs of thickness 0.5 mm with corresponding masses about 12.00 mg.

#### 3.2. Dynamic ADSC modulated temperature programmes

The heat flow, heat capacities and phase angle measurements were obtained using the Mettler–Toledo DSC 820 equipped with an intracooler and ADSC evaluation was performed using STAR<sup>®</sup> software version 3.0.

Every dynamic ADSC curve was run from 80 to 180°C with an average heating rate of 0.5°C/min, following a conventional DSC programme of heating to 180°C at 10°C/min and cooling from 180 to 80°C at –20°C/min in order to erase the previous thermal history of the samples. The modulation amplitudes  $A_T$  were either 0.5 or 1 K; the periods were varied between 12 s and 240 s. The intracooler was run during all the measurements and nitrogen with a flow rate of 80 ml/min was used as the purge gas.

#### 3.3. ADSC evaluation

Three separate ADSC runs were performed for each evaluation:

1. Empty run – without crucibles in either sample or reference positions;
2. Blank run – a crucible with lid in the sample position and a crucible without lid in the reference position;
3. Sample run – polycarbonate sample in the same crucible and with the same lid (as for 2) in the sample position and the same crucible without lid (as for 2) in the reference position.

The empty and blank runs are used for the calibration of the DSC cell and for compensation of the cell asymmetry. The Mettler–Toledo STAR<sup>®</sup> software

was used for ADSC evaluation, from which heat flow (HF), complex heat capacity ( $C_p^*$ ), in-phase heat capacity ( $C_p'$ ), out-of-phase heat capacity ( $C_p''$ ) and phase angle ( $\phi$ ) can be obtained. It should be noted that the phase angle evaluated by the Mettler–Toledo analysis is negative in the glass transition region, indicating that the heat flow modulations lag behind the heating rate modulations.

### 4. Results and discussion

The dynamic ADSC measurements shown in Fig. 2 for a sample mass of 11.80 mg encompass the glass transition region of polycarbonate and can be quantified by a number of features, defined by reference to Fig. 3. The important features selected here are  $T_{\text{mid}}$ ,  $\Delta C_p^*$ ,  $\phi$  at 100°C,  $\Delta\phi$  and  $\Delta\phi_{\text{max}}$ . The results are summarised in Table 1.

The magnitude of the phase angle is critical to the evaluation of the in-phase and out-of-phase components of  $C_p^*$  (refer to Eqs. (4) and (5)). The dependence of the phase angle on frequency, illustrated by these results, is therefore very interesting. First of all, it is clear that the phase angle in the glassy state, quantified by  $\phi$  at 100°C, is not zero as anticipated theoretically in the absence of heat transfer effects [5,6]. Its dependence on frequency, though, shown in Fig. 4, shows an approximately linear relationship (dashed line) in accordance with the approximation of Eq. (10) for small phase angles [7]. It would appear appropriate, therefore, to make a correction of the phase angle to zero in this glassy region in order to allow for the effects of heat transfer; this correction will increase with frequency. It may also be noted that Eq. (10) predicts a linearly increasing phase angle as the specific heat capacity increases. Since it can be seen that the glassy specific heat capacity increases approximately linearly with temperature (refer to Fig. 2) and by about 15% over the whole of the temperature range used here (80°C to 180°C), one would anticipate a similar increase in the (negative) phase angle. A line with this slope is drawn tangentially to the phase angle curve in Fig. 2, from which it can be seen that this correspondence is reasonably well followed by these results.

The second important aspect of these phase angle results relates to what happens in the transition region.

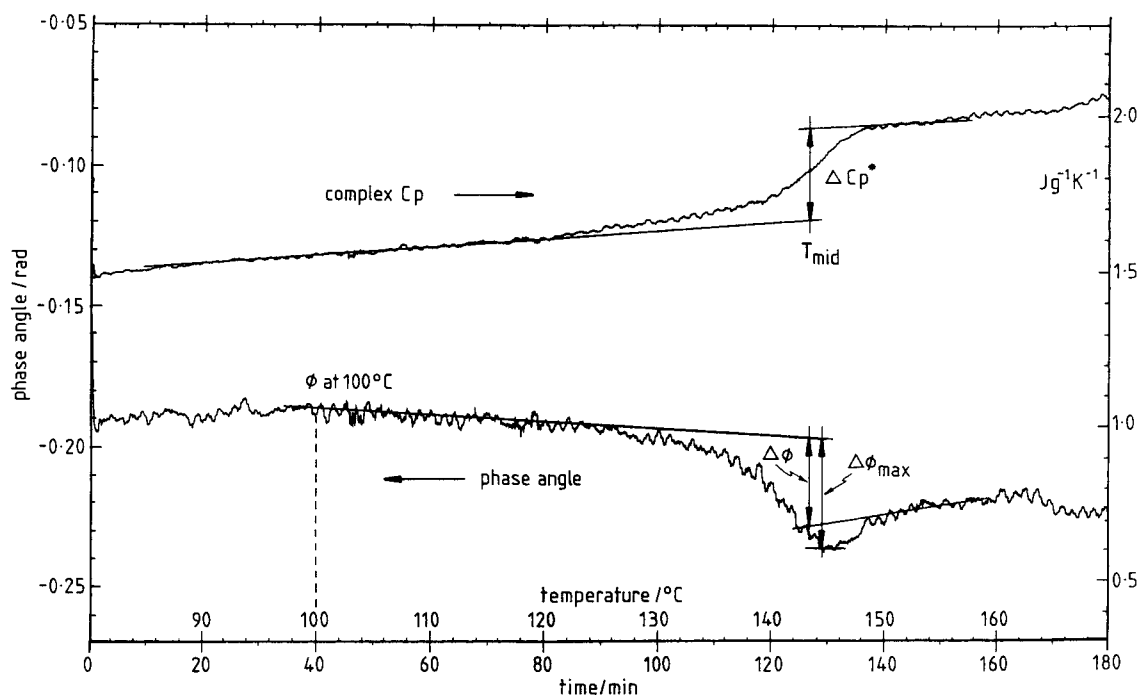


Fig. 3. Illustration of the measurement of the characteristic features of the ADSC scan in the glass transition region.

Table 1  
Results of dynamic ADSC through  $T_g$  region

Amplitude K	Period min	$T_{mid}$ °C	$\Delta C_p^*$ J/g K	$\Delta C_p'$ J/g K	$\Delta C_p''$ J/g K	$\phi$ at 100°C rad	$\Delta\phi$ rad	$\Delta\phi_{max}$ rad	$\Delta\phi_{max}(corr)$ rad
0.5	0.2	137.3	0.22	0.18	-0.19	-0.366	0.050	0.053	0.012
0.5	0.4	138.6	0.31	0.27	-0.16	-0.354	0.027	0.032	0.006
0.5	0.6	145.7	0.15	0.12	-0.12	-0.295	0.026	0.032	0.012
0.5	0.8	143.6	0.19	0.18	-0.09	-0.223	0.024	0.032	0.018
0.5	1	144.5	0.22	0.21	-0.08	-0.200	0.015	0.022	0.010
0.5	1.6	143.4	0.23	0.22	-0.07	-0.168	0.012	0.033	0.024
0.5	2	142.7	0.22	0.21	-0.07	-0.120	0.008	0.036	0.026
0.5	3	142.0	0.22	0.21	-0.04	-0.063	0.005	0.035	0.028
0.5	4	142.4	0.22	0.21	-0.03	-0.034	0.003	0.031	0.026
1	0.2	154.7	0.17	0.14	-0.08	-0.286	0.062	0.071	0.034
1	0.4	147.1	0.18	0.16	-0.11	-0.308	0.033	0.044	0.020
1	0.6	145.3	0.17	0.14	-0.11	-0.280	0.041	0.042	0.016
1	0.8	146.1	0.18	0.16	-0.10	-0.270	0.030	0.038	0.020
1	1	145.2	0.19	0.17	-0.10	-0.187	0.025	0.040	0.027
1	1.6	143.4	0.20	0.19	-0.09	-0.170	0.023	0.041	0.026
1	2	143.1	0.20	0.19	-0.06	-0.106	0.017	0.041	0.030
1	3	142.1	0.20	0.19	-0.03	-0.062	0.012	0.039	0.030
1	4	142.6	0.21	0.20	-0.02	-0.040	0.008	0.040	0.032

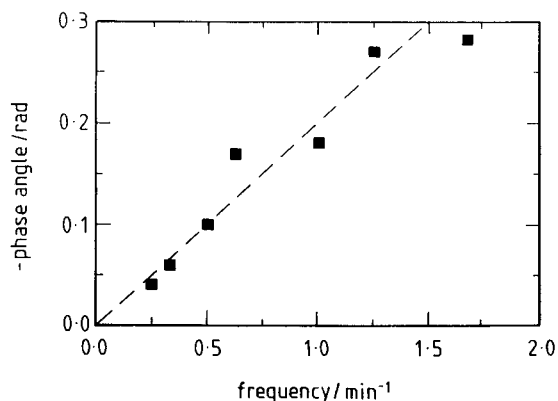


Fig. 4. Dependence of (negative) phase angle at 100°C (i.e. in glassy state) on frequency for polycarbonate (11.80 mg) evaluated by dynamic ADSC with an amplitude  $A_T=1.0$  K and an average heating rate  $\beta=0.5$  K/min. The dashed line represents the relationship between  $\phi$  and  $\omega$  defined by Eq. (10).

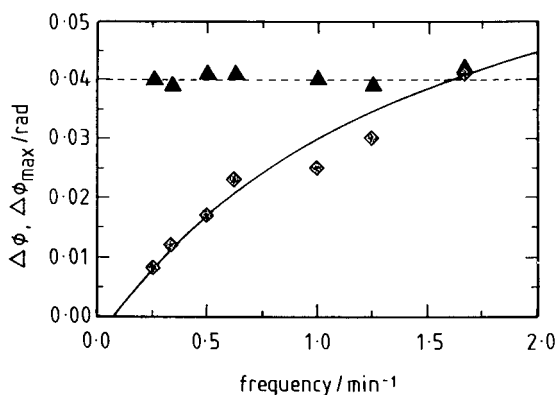


Fig. 5. Dependence of  $\Delta\phi$  (full line) and  $\Delta\phi_{\max}$  (dashed line) on frequency for polycarbonate in the glass transition region by dynamic ADSC with  $\beta=0.5$  K/min and  $A_T=1.0$  K. The full and dashed lines are drawn to guide the eye.

There are two features of note: the increment  $\Delta\phi$  and the maximum departure  $\Delta\phi_{\max}$  (Fig. 3), the dependence of each of these on frequency being shown in Fig. 5. There is an obvious increase of  $\Delta\phi$  with frequency, but in this case there is a well defined non-linearity. Furthermore, a reasonable extrapolation to zero frequency without the occurrence of any reversed curvature would yield a change in sign of  $\Delta\phi$  for periods of the order of 10 min and greater. This unexpected behaviour has been further verified in quasi-isothermal experiments [8] in respect of the phase angle itself,  $\phi$  at 100°C; quasi-isothermal

experiments ( $\beta=0$ ) have an advantage here since increasingly long periods in dynamic ADSC experiments require a continued reduction in the average heating rate in order to accommodate sufficient periods within the transition region.

In contrast to  $\Delta\phi$ , the maximum departure  $\Delta\phi_{\max}$  remains rather constant with frequency, at an average value of 0.040 rad for the amplitude of 1.0 K and 0.032 rad for the amplitude of 0.5 K.

The implications of these observation for 'real' phase angles in the glass transition region can now be considered. Consider the changes in the phase angle that are experimentally measured in the transition region during two typical ADSC scans, one at 'high frequency' (e.g. period of 36 s,  $\omega=0.17$  rad s $^{-1}$ ) and the other at 'low frequency' (e.g. period of 4 min,  $\omega=0.03$  rad s $^{-1}$ ). The measured glassy state phase angles will be different in each case, being dependent on the frequency (Fig. 4), but may be corrected to zero, as discussed above, in accordance with the theoretically anticipated result. This correction would leave the (negative) phase angle variations with temperature illustrated schematically in Fig. 6: at high frequency, the increment in  $\phi$  on going through the transition,  $\Delta\phi$ , is larger than that for low frequency, whereas the maximum departure  $\Delta\phi_{\max}$  remains rather constant with frequency, in accordance with the results shown in Fig. 5.

Recalling now that, to a first approximation, the phase angle at constant frequency is proportional to  $C_p$  (Eq. (10)) and following the suggestion of Weyer et al. [9], we may ascribe the increment in  $\phi$  at the transition to the increment in  $C_p$  (refer to  $C_p^*$  trace in Fig. 2). The baseline for the correction of the phase angle will therefore be a sigmoidal curve which mirrors the change in  $C_p^*$  with temperature in the transition region, but which is scaled by the frequency; these baselines are shown in Fig. 6 as dashed and dotted lines for high and low frequency, respectively. The full correction of the phase angle would therefore include not only that already made to set the value to zero in the glassy state, but also the subtraction of the dashed/dotted baselines in Fig. 6 to result in zero phase angle in the liquid-like state, again as anticipated theoretically [5,6]. The phase angle data for polycarbonate shown in Fig. 3 have been corrected following the above procedure and the corrected curve for the (negative) phase angle is shown in Fig. 7.

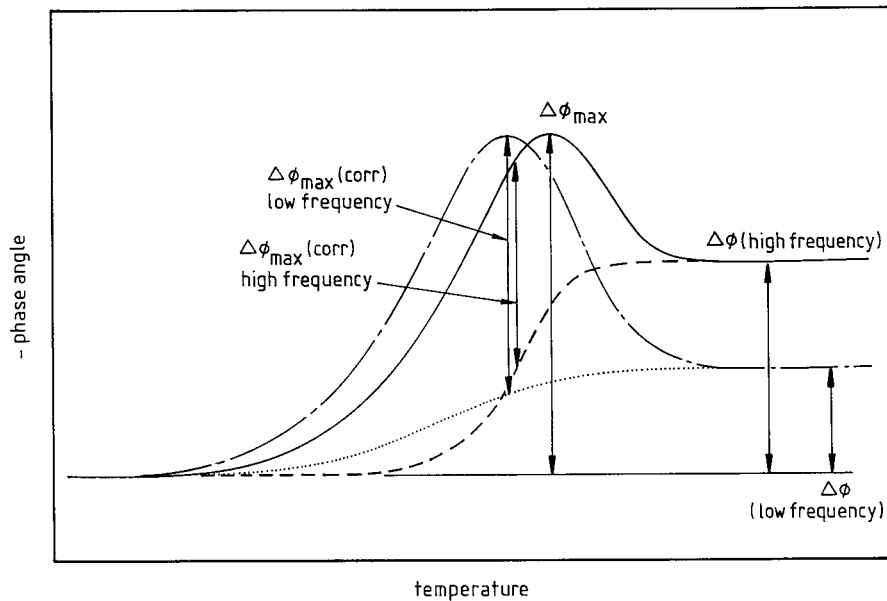


Fig. 6. Schematic illustration of the correction of the (negative) phase angle to allow for heat transfer effects. Two curves are shown, one for high frequency (full line) and the other for low frequency (dash-dotted line), both with phase corrected to zero in the glassy state. For each, a baseline (dashed and dotted line, respectively) is drawn, following the scaled complex heat capacity trace for each frequency. Note that the high frequency curve and baseline are shifted slightly to the right (higher temperatures) relative to the low frequency curve and baseline, following the dependence of  $T_{mid}$  on frequency (refer to Table 1); this will have no effect on the arguments advanced here.

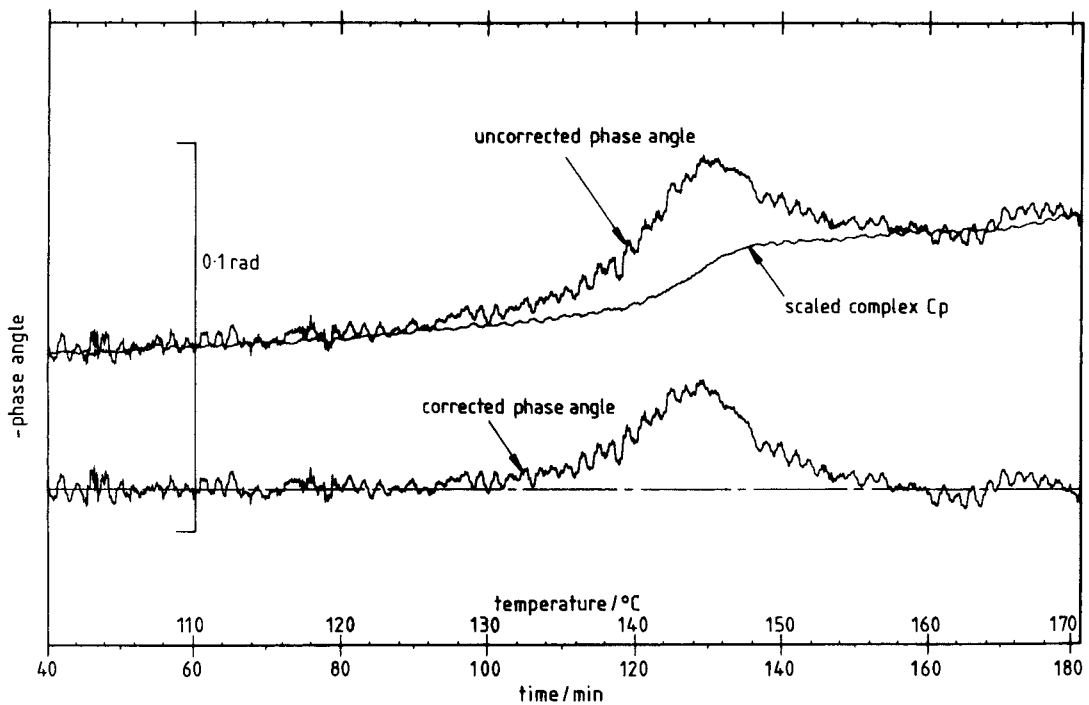


Fig. 7. Uncorrected and corrected (negative) phase angle for polycarbonate from Fig. 3, following the procedure outlined in the text.

Table 2

Predictions of the single relaxation time model [5,6,10] for the effects of period and amplitude of modulation on the maximum departure of the phase angle in the glass transition region. The initial enthalpy at  $T_g - 10$  K at the start of the ADSC scan has a value of 3.0 J/g, which corresponds to an instantaneous quench to this temperature from equilibrium at  $T_g$ .

$\beta$ , K/min	period, s	$A_T$ , K	$\Delta\phi_{\max}$ , rad
0.5	30	0.25	0.11
0.5	60	0.25	0.12
0.5	120	0.25	0.16
0.5	60	0.25	0.12
0.5	60	0.50	0.12
0.5	60	0.75	0.12
2.0	60	0.25	0.36
2.0	60	0.50	0.24
2.0	60	0.75	0.21

This correction procedure, suggested by Weyer et al. [9], has some interesting implications, in particular for  $\Delta\phi_{\max}$ . It can be seen from Fig. 6 that although  $\Delta\phi_{\max}$  measured experimentally appears to remain rather constant, its value when corrected for the frequency effects of heat transfer,  $\Delta\phi_{\max}$  (corr), decreases with increasing frequency (or increases with increasing period of modulation). The data in Table 1 confirm this trend. Exactly this dependence of phase angle on frequency or period in the glass transition region has also been predicted by the improved solution [10] to the original theoretical model [5,6], for which some results are summarised in Table 2. From the first set of results presented in the table, it can be seen that  $\Delta\phi_{\max}$  increases with increasing period.

The corresponding effect of the amplitude of modulation on  $\Delta\phi_{\max}$  is not so easy to compare. The experimental results (Table 1) show that both  $\Delta\phi_{\max}$  and  $\Delta\phi$  increase with increasing amplitude of modulation, so that the corrected value of  $\Delta\phi_{\max}$  following the procedure outlined above will depend upon  $A_T$  in a way that is determined by the relative rates of increase of  $\Delta\phi_{\max}$  and  $\Delta\phi$  with  $A_T$ . The second and third sets of theoretical results in Table 2 suggest that the effect of  $A_T$  on  $\Delta\phi_{\max}$  (corr) could depend also on the choice of experimental variables, i.e. of  $\beta$  or, presumably, the period.

The procedure suggested by Schick and co-workers [9] for the correction of the phase angle to allow for

the instrumental effects is therefore supported by the results presented here and appears as a logical and rational approach to this problem. The corrected phase angle will enable the in-phase and out-of-phase components of  $C_p^*$  to be calculated more realistically than has hitherto been possible, particularly in the latter case for which the interpretation of the significance of  $C_p''$  remains somewhat unclear.

## 5. Conclusions

The experimental results show some important characteristic features of the phase angle in dynamic ADSC in the glass transition region. In the glassy state, the phase angle is not zero, but depends approximately linearly on the frequency, as is anticipated theoretically to a first approximation from an analysis of heat transfer. In the liquid-like state above  $T_g$ , the phase angle is again non-zero, but now incremented relative to the glassy state value and is again frequency dependent. This increment is attributed to the change in specific heat capacity at  $T_g$ , as anticipated theoretically. These observations are consistent with the phase angle correction procedure suggested by Schick and co-workers, whereby a baseline corresponding to the complex heat capacity trace is subtracted from the experimental phase angle trace. The resulting corrected phase angles, in particular the maximum departures in the transition region, are shown to agree with the predictions of a simple model for the response of a glass to alternating DSC in the glass transition region.

## Acknowledgements

We are grateful to Mettler–Toledo and Aberdeen University Research Committee for financial support of this project.

## References

- [1] J.C. Seferis, I.M. Salin, P.S. Gill, M. Reading, Proc. Acad. Greece 67 (1992) 311.
- [2] P.S. Gill, S.R. Sauerbrunn, M. Reading, J. Thermal Anal. 40 (1993) 931.
- [3] M. Reading, D. Elliott, V.L. Hill, J. Thermal Anal. 40 (1993) 949.



- [4] J.E.K. Schawe, Thermochim. Acta 260 (1995) 1.
- [5] J.M. Hutchinson, S. Montserrat, J. Thermal Anal. 47 (1996) 103.
- [6] J.M. Hutchinson, S. Montserrat, Thermochim. Acta 286 (1996) 263.
- [7] B. Wunderlich, Y. Jin, A. Boller, Thermochim. Acta 238 (1994) 277.
- [8] Z. Jiang, C.T. Imrie, J.M. Hutchinson, Part 2 of this series, to be published.
- [9] S. Weyer, A. Hensel, C. Schick, Thermochim. Acta, 304/305 (1997) 267.
- [10] J.M. Hutchinson, S. Montserrat, Thermochim. Acta, 304/305 (1997) 257.